

SEASONAL OCEANIC HEAT TRANSPORTS COMPUTED FROM AN ATMOSPHERIC MODEL

GARY L. RUSSELL¹, JAMES R. MILLER² and LIE-CHING TSANG³

¹ *NASA-Goddard Space Flight Center, Institute for Space Studies, 2880 Broadway, New York, NY 10025 (U.S.A.)*

² *Department of Meteorology and Physical Oceanography, Cook College, Rutgers, The State University of New Jersey, New Brunswick, NJ 08903 (U.S.A.)*

³ *M/A-COM Sigma Data, Inc., 2880 Broadway, New York, NY 10025 (U.S.A.)*

(Received December, 1984; revised April 15; accepted April 17, 1985)

ABSTRACT

Russell, G.L., Miller, J.R. and Tsang, L.-C., 1985. Seasonal oceanic heat transports computed from an atmospheric model. *Dyn. Atmos. Oceans*, 9: 253–271.

Seasonal estimates of the oceanic poleward heat transport are obtained using a climate model that is a global atmospheric general circulation model on an $8^\circ \times 10^\circ$ grid. The climate model is used to calculate the surface heat flux into each ocean grid point for each day of the year. The rate of ocean heat storage is calculated using climatological surface temperatures, mixed layer depths, and ice amounts. By assuming that the rate of change of heat storage in the deep ocean is spatially constant, the horizontal transports are calculated from the vertical fluxes and the upper ocean storage rates. The oceanic meridional transports for each latitude and for each ocean basin are derived, and results are compared with other calculations of the seasonal transports. In the Northern Hemisphere, comparisons between the simulated seasonal transports indicate that the annual variation is much greater in the Pacific than in the Atlantic.

1. INTRODUCTION

A poleward transport of heat by the atmosphere and oceans is required to maintain a global steady state heat balance. A number of recent studies have contributed to a better understanding of the ocean's role in this process. These are described in a comprehensive review by Bryan (1982a). Knowledge of these transports is important for understanding climate and climatic variations.

There are a number of different methods for calculating ocean heat transports. These include direct methods based on hydrographic data, indirect methods based on surface heat flux calculations from observations or

from atmospheric general circulation models, residual methods based on satellite and atmospheric data, and heat transports calculated from numerical ocean models. These methods and some of the studies using them are described briefly in Miller et al. (1983, hereinafter referred to as MRT) and in greater detail in Bryan (1982a). Most of these studies included calculation of annual global transports across different latitudes.

The purpose of this paper is to extend the results of MRT by calculating the seasonal oceanic meridional heat transports and comparing them with the annual values given in MRT. Other calculations of the annual ocean transports using an atmospheric model have been done by Slingo (1982). The method is equivalent to the indirect method with the surface heat flux data generated by an atmospheric general circulation model tailored for climate studies. Several additional assumptions are required.

The surface heat fluxes from a 1-y simulation of the climate model are saved for each day and for each ocean grid point. The rate of heat storage between the surface and the annual-maximum mixed-layer depth is calculated from climatological data. It is assumed that the mixed layer temperature is uniform, that the temperature of the water between the mixed layer and its annual maximum does not change in time, and that the ocean ice depths can be derived from their horizontal extent. The rate of change of heat storage in the deep ocean is assumed to be spatially uniform, and is equal to the global surface heat flux minus the global energy stored in the upper ocean. The converged horizontal transports are calculated from the surface heat fluxes and the ocean storage. By integrating the converged horizontal transports for each ocean basin from the North Pole to a particular latitude, the meridional transports are obtained.

2. CALCULATION OF THE SEASONAL OCEANIC HEAT TRANSPORT

The climate model used to calculate the vertical heat flux into the ocean has been described by Hansen et al. (1983) and is the same as that used in MRT. The model has $8^\circ \times 10^\circ$ horizontal resolution and nine vertical layers. Source terms include a comprehensive radiation package and parameterization of condensation and surface interaction. The model's ability to simulate the net radiational heating at the top of the atmosphere, the divergence of static energy flux and surface heat flux has been discussed in MRT. Diagnostics for all ocean grid boxes were saved and were used to calculate the oceanic heat transports.

For each grid box, the surface flux, the converged oceanic transport of heat, and the time change of energy satisfy the equation

$$VF + OT = \frac{\partial EU}{\partial t} + \frac{\partial ED}{\partial t} \quad (1)$$

where VF (W m^{-2}) is the vertical flux of heat from the atmosphere into the ocean and was saved from a run of the climate model, OT (W m^{-2}) is the converged horizontal transport, EU and ED (J m^{-2}) are the thermal energy of the upper and deep ocean, and t is time. In this paper, the term “upper ocean” refers to the ocean between the surface and the annual-maximum mixed-layer depth. The term “deep ocean” refers to the ocean below the annual-maximum mixed-layer depth.

The vertical heat flux into the ocean and ocean ice is calculated by the climate model from the equation

$$VF = SR - TR - SH - LH + PR \quad (2)$$

where SR is the net downward solar radiation, TR is the net upward thermal radiation, SH is the upward sensible heat flux, LH is the upward latent heat flux from evaporation (negative for dew), and PR is the precipitation heat flux (negative for snow).

Using brackets to represent an annual average and an overbar a spatial average, $[\overline{VF}]$ was 4.0 W m^{-2} for the 1 y run. As discussed in MRT, a constant factor $x = 0.9776$ was introduced to normalize the solar radiation so that $[\overline{VF^x}] = 0$ where

$$VF^x = x \cdot SR - TR - SH - LH + PR \quad (3)$$

If atmospheric storms cross a grid box, large temporal variations in the vertical flux occur. Figure 1 shows the daily average of VF^x at Ocean Station Papa (145°W , 50°N) in the North Pacific for a 1-y run. One way to calculate the model’s climatological vertical transports is to integrate the climate model for many years and average the daily vertical fluxes over those

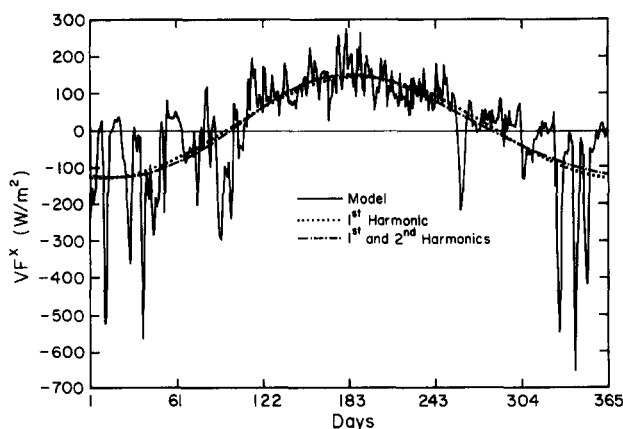


Fig. 1. Vertical heat flux into the ocean at Ocean Station Papa (145°W , 50°N) as calculated from the climate model.

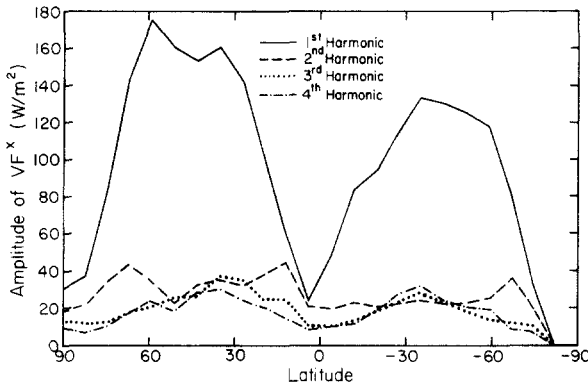


Fig. 2. Amplitude of the first four harmonics of vertical heat flux as a function of latitude.

years. That is expensive in computing time. The method chosen here is to fit the model's vertical fluxes with the annual average and the first few temporal harmonics at each grid box. Figure 2 shows that in the mid-latitudes, the amplitude of the first harmonic is five times larger than the amplitude of any other harmonic. It also shows that in the tropics and in high latitudes where ocean ice occurs, the second harmonic is twice as large as the third harmonic.

Although it may be important to include higher harmonics to obtain monthly averages of the heat transports, our calculations indicate that the contribution of the second harmonic to the seasonal transports is small. We have therefore chosen to use the annual average and the first temporal harmonic in all subsequent calculations.

The energy of the upper ocean and ocean ice is determined from monthly values of three observed quantities: the ocean surface temperature, the mixed-layer depth, and the horizontal ice coverage. The mixed-layer depths were calculated from bathythermograph data obtained from the National Oceanographic Data Center (NODC) and are described in section 4. Because observations of ice depths are sparse, it was necessary to determine depths from the horizontal coverage. For each grid box, N is the number of months when some ice is present. The ice depth Z (m) is set equal to $1 + R\sqrt{N}$ where R is the ratio of ocean ice area to total ocean area of a grid box. If $N = 12$, the depth is set equal to $1 + 4R$. Hence, the ice depths vary seasonally and spatially, but are always between 1 and 5 m. They may be too deep in the Southern Hemisphere (Gordon, 1982).

The average temperature of the mixed layer is assumed to be equal to the ocean surface temperature. When the mixed layer becomes shallower, the temperature profile in the layer between the mixed layer depth and its annual-maximum is saved so that thermal energy is conserved. When the mixed layer deepens there is no change in the temperature profile below the

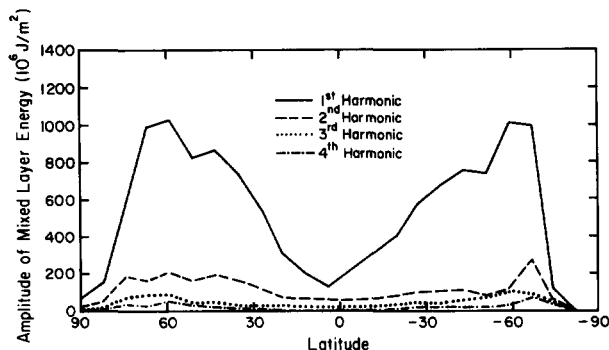


Fig. 3. Amplitude of the first four harmonics of upper ocean energy as a function of latitude.

mixed layer. Thus, starting from the day on which the mixed layer is at its maximum, we can integrate in time and calculate the upper ocean thermal energy for each day. The mixed-layer depths are updated daily using the monthly climatology calculated from the NODC data. Figure 3 shows the variation with latitude of the magnitude of the first four harmonics of upper ocean energy. In subsequent calculations, E is fitted by its annual average and first harmonic.

By averaging eq. 1 over the whole globe, the horizontal ocean transports cancel, and we are left with

$$\overline{VF^z} = \frac{\partial \overline{EU}}{\partial t} + \frac{\partial \overline{ED}}{\partial t} \quad (4)$$

Since the first two quantities are known, the time rate of change of global heat storage in the deep ocean can be calculated. It is shown in Fig. 4. Note that during the second quarter, there is a global downward transport into the deep ocean.

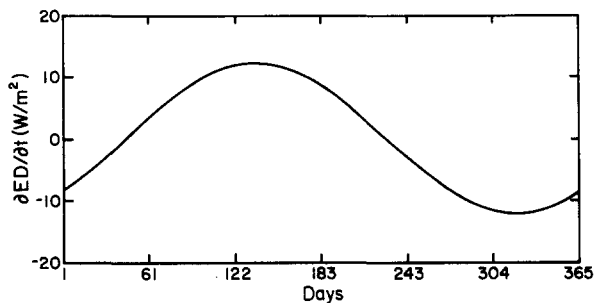


Fig. 4. Annual cycle of the time rate of change of deep ocean energy for the global ocean using the first harmonic of vertical flux and upper ocean energy.

To calculate the seasonal meridional heat transports, some assumption about the spatial distribution of heat storage in the deep ocean must be made in the absence of actual data. We chose to use the simplest assumption which is that the time rate of change of heat storage in the deep ocean is uniformly distributed in space. All subsequent calculations will therefore assume that $\partial ED/\partial t$ is spatially uniform, and therefore for each instant in time

$$\frac{\partial ED}{\partial t} = \frac{\partial \overline{ED}}{\partial t} \quad (5)$$

We reiterate that this assumption does affect the transports, and in the future it should be replaced using climatological deep ocean data.

With the assumption, the seasonal horizontal ocean transports are obtained from eqs. 1 and 5 as

$$OT = \frac{\partial EU}{\partial t} + \frac{\partial \overline{ED}}{\partial t} - VF^x \quad (6)$$

Averaging over an annual cycle, $\partial EU/\partial t$ and $\partial \overline{ED}/\partial t$ disappear, and we are left with

$$[OT] = -[VF^x] \quad (7)$$

Equation 7 was used to calculate the annual oceanic meridional heat transports in MRT. The seasonal transports are calculated in this paper by integrating eq. 6 over the area from a particular latitude, ϕ , to the North Pole

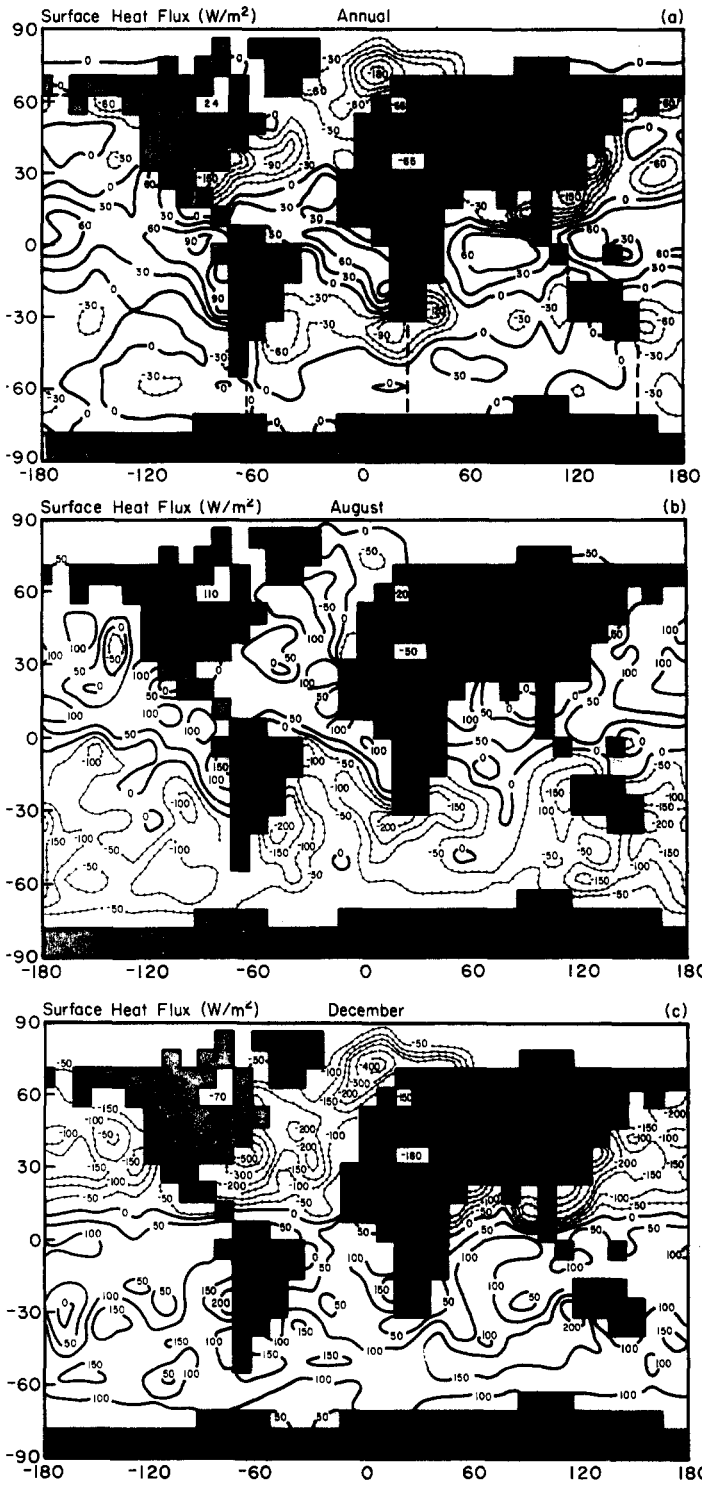
$$Q_\phi = \int_\phi^{90^\circ N} OT \, dA \quad (8)$$

where $Q_\phi(W)$ is the northward transport of energy across a particular latitude. Equation 8 can be calculated separately for each basin or averaged in time to obtain the transports for a particular season.

3. SEASONAL CHANGES IN SURFACE HEAT FLUXES

As discussed in the previous section, seasonal oceanic meridional heat transports calculated from the climate model depend on the seasonal variations of the surface heat fluxes and the ocean heat storage. Assuming that there is no net oceanic heat storage over an annual cycle, only the net annual surface heat fluxes are needed when calculating the annual meridional

Fig. 5. Model calculated surface heat flux into the ocean for (a) the annual average (b) August and (c) December.



transports. Since we are concerned here with seasonal transports, it is useful to first discuss seasonal variations of the surface heat fluxes.

Figure 5 shows the annual, August and December surface heat fluxes generated by the climate model. The annual fluxes were used to calculate the annual meridional heat transports in MRT. In the summer hemisphere there is a net flux of heat into the ocean nearly everywhere. In the winter hemisphere, the heat fluxes are negative outside the tropics and are quite large in mid-latitudes in the areas of the strong western boundary currents. The negative heat fluxes in the winter hemisphere are accompanied by a cooling of the ocean mixed layer and hence a reduction in the ocean heat storage.

Figure 6 shows observed values of the heat flux in the Pacific for August and December. These 20-y averages were calculated by Weare (1983). The model reproduces a number of features of the observed August climatology including the zero contour at ~ 5 to 10°S and the positive fluxes extending southward along the South American coast. There are also significant differences. The observed heat fluxes in the Northern Hemisphere are nearly uniform at 50 W m^{-2} . In August for both hemispheres, the model shows much greater variability and generally larger magnitudes.

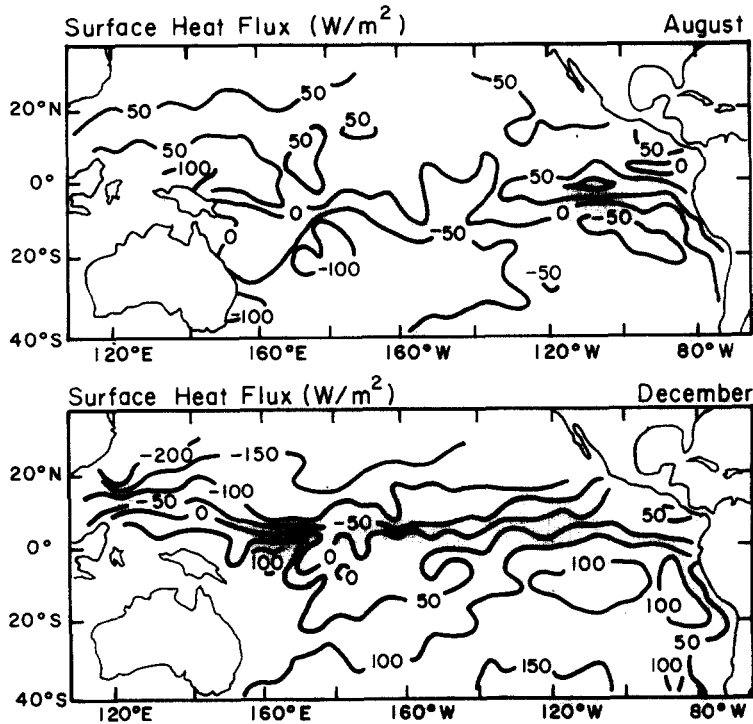


Fig. 6. Observed surface heat flux for August and December in the Pacific (Weare, 1983).

The results for December show that both the model and the observations yield zonal patterns in the Northern Hemisphere, but greater zonal variability in the Southern Hemisphere. In both hemispheres, the magnitudes of the model and observed fluxes are in good agreement. The annual fluxes compare favorably with observations as shown in MRT.

4. SEASONAL CHANGES IN OCEAN HEAT STORAGE

Seasonal variations of meridional oceanic heat transports depend critically on how heat is stored in the ocean. If the surface heat fluxes are assumed to be uniformly distributed through the mixed layer, then the amount of heat that can be stored for a realistic temperature distribution depends on the depth of the mixed layer. To account accurately for changes of ocean heat storage, we have chosen to allow the ocean mixed-layer depth to vary according to climatology at each grid point. Using all the bathythermograph data from NODC, each mixed-layer depth was assumed to be the shallowest depth at which the temperature is 0.5°C less than the surface temperature, but each depth was limited to 250 m. These depths were then binned into months and spatially smoothed. Figure 7 shows the calculated mixed-layer depths for February and August. The minimum depth at any grid box at any time is 17 m.

The upper ocean heat content, EU , is given by

$$EU = \rho_w c_w \int_{-h}^0 T(z) dz + \rho_i z_i (-L + c_i T_i - c_w T(0)) \quad (9)$$

where ρ_w and ρ_i are densities of water and ice, c_w and c_i are specific heats of water and ice, h is the annual-maximum mixed-layer depth, T is water temperature as a function of depth, T_i is ice temperature, z is the variable water depth, z_i is the ice depth, and L is the latent heat of melting. Because of lack of temperature data below the surface, the calculation of heat storage for this paper uses only the mixed-layer depths and the surface temperatures. The algorithm to determine EU from those two quantities and the ice data is given in section 2.

Figure 8 shows the ocean energy at Ocean Station Papa over an annual cycle. The observed energy is a 10-y average (1958–1967) based on the data of Ballis (1973) using depths to 250 m. The calculated annual-maximum mixed-layer depth at Ocean Station Papa is 150 m which explains the discrepancy in the energy values. The annual variation of the heat storage is reasonably well calculated using the EU algorithm, although there does appear to be a phase shift of less than 1 month. Both the maximum and the minimum occur nearly 1 month later than the observed.

The amplitudes of the annual cycle of heat content change will be greatest

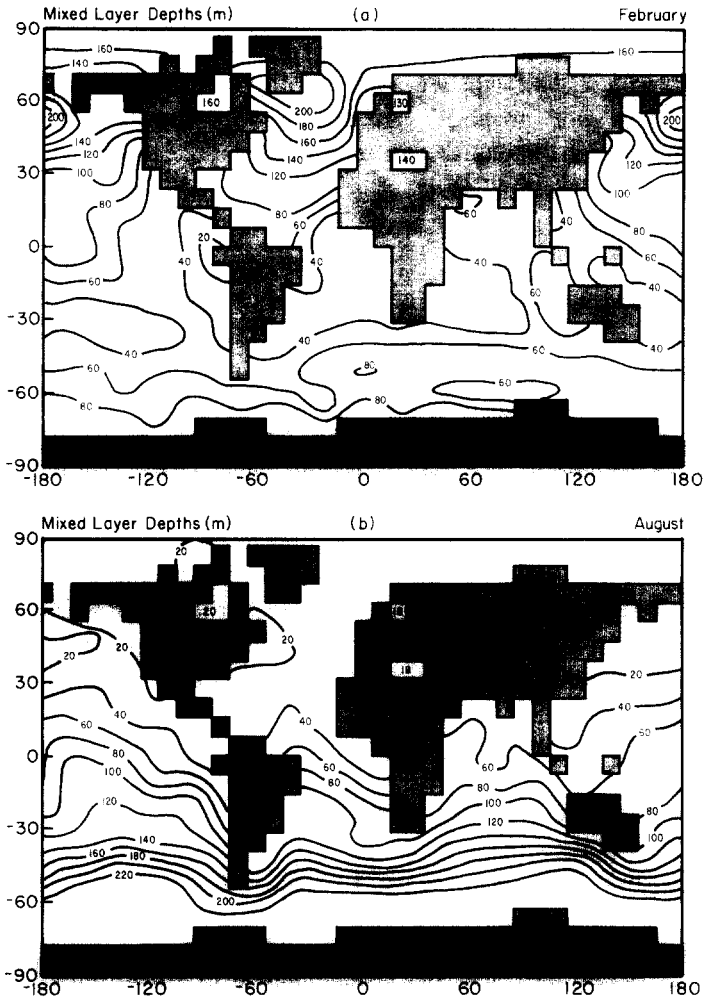


Fig. 7. Mixed-layer depths for (a) February and (b) August.

in regions where the maximum variations in mixed-layer depths occur. Hence the maximum amplitudes of the annual heat content changes should occur at mid-latitudes, whereas in the tropics the amplitudes should be smaller. The amplitude for the ocean energy is shown in Fig. 3.

The rate of heat storage, $\partial EU/\partial t$, is an important variable when determining the meridional ocean heat transport. Figure 9 shows the rate of heat storage for the first quarter of the year as fitted by the first harmonic. The storage for the third quarter is the same as that for the first quarter but has the opposite sign. As expected, the rate of heat storage is positive in the summer hemisphere and negative in the winter hemisphere. The maximum

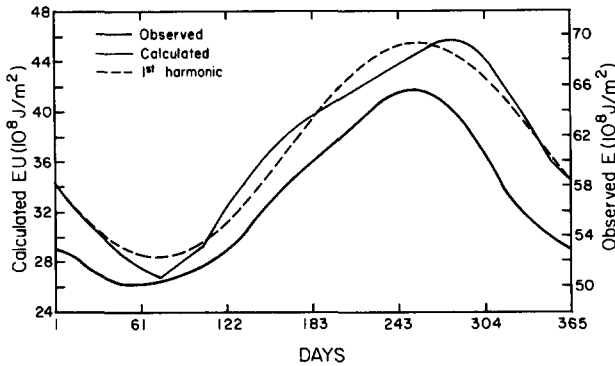


Fig. 8. Upper ocean energy at Ocean Station Papa as calculated by the model using climatologically varying mixed-layer depths and temperatures and comparisons with the observed values.

rates in the Northern Hemisphere are associated with the western boundary currents and the very high latitude region to the east of Greenland. In the Southern Hemisphere, the maximum rates of heat storage occur at about 60°S . As shown in Fig. 7 some of the deepest mixed-layer depths occur in this region and such depths would lead to the large rate of heat storage.

Figure 10 shows the rate of heat storage in oceans as calculated from observations in the Northern Hemisphere by Oort and Vonder Haar (1976), as computed from the ocean model of Meehl et al. (1982) and as computed

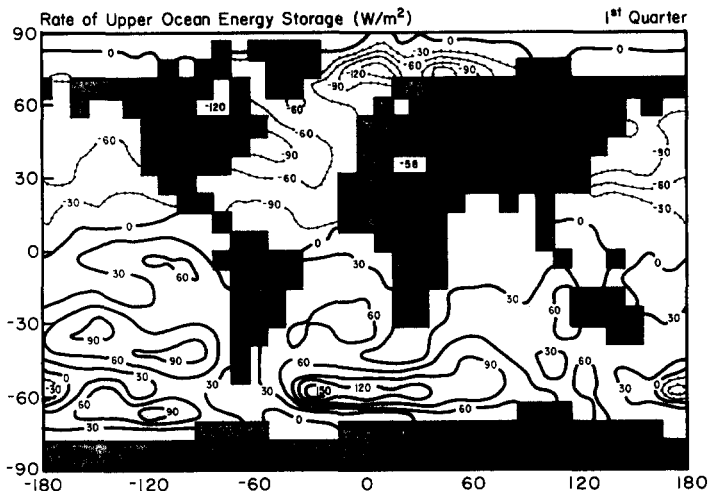


Fig. 9. Rate of upper ocean energy storage using the first harmonic for the January to March quarter.

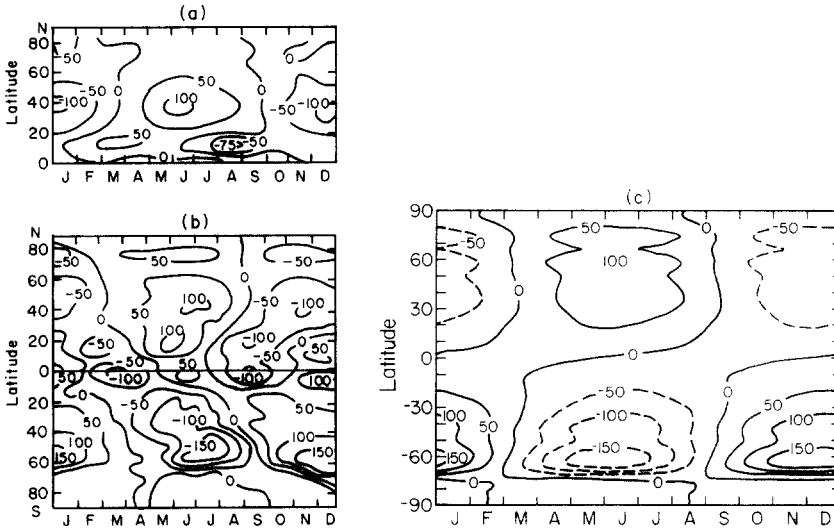


Fig. 10. Annual cycle of rate of heat storage (W m^{-2}) as calculated by (a) Oort and Vonder Haar, 1976 (b) Meehl et al., 1982 and (c) the climate model. The ocean values are obtained by dividing by the fraction of ocean at each latitude.

from the present model. To obtain the actual ocean values, one must divide by the ocean fraction at each latitude. Meehl et al. also showed a Southern Hemisphere maximum between 50 and 60°S which is consistent with the present model. Comparisons of these three different calculations show that the present model is in reasonably good agreement with the other values.

5. SEASONAL CHANGES IN MERIDIONAL OCEANIC HEAT TRANSPORT

Figure 11a from MRT shows the annual oceanic heat transport for each of the three ocean basins and for the global ocean. The global heat transport is poleward in both hemispheres with maximum transports near 20° . For the global ocean, the residual at the Antarctic continent is zero, a result that must occur under the assumption of no net annual heat storage. However, for the individual basins, the residuals are 1.35 PW, -1.1 PW and -0.25 PW for the Atlantic, Pacific and Indian Oceans, respectively. (1 PW = 1 petawatt = 10^{15} W.) Positive values at Antarctica indicate a net transport of heat into a basin. The transports of the Atlantic and Pacific basins are quite different. The heat transport in the Pacific is poleward in both hemispheres, but in the Atlantic the transport is everywhere northward.

Seasonal meridional transports have been calculated for each ocean basin and the global ocean using eq. 8. Figure 11b–e shows the results for each quarter of the year. These can be compared with the annual values in Fig.

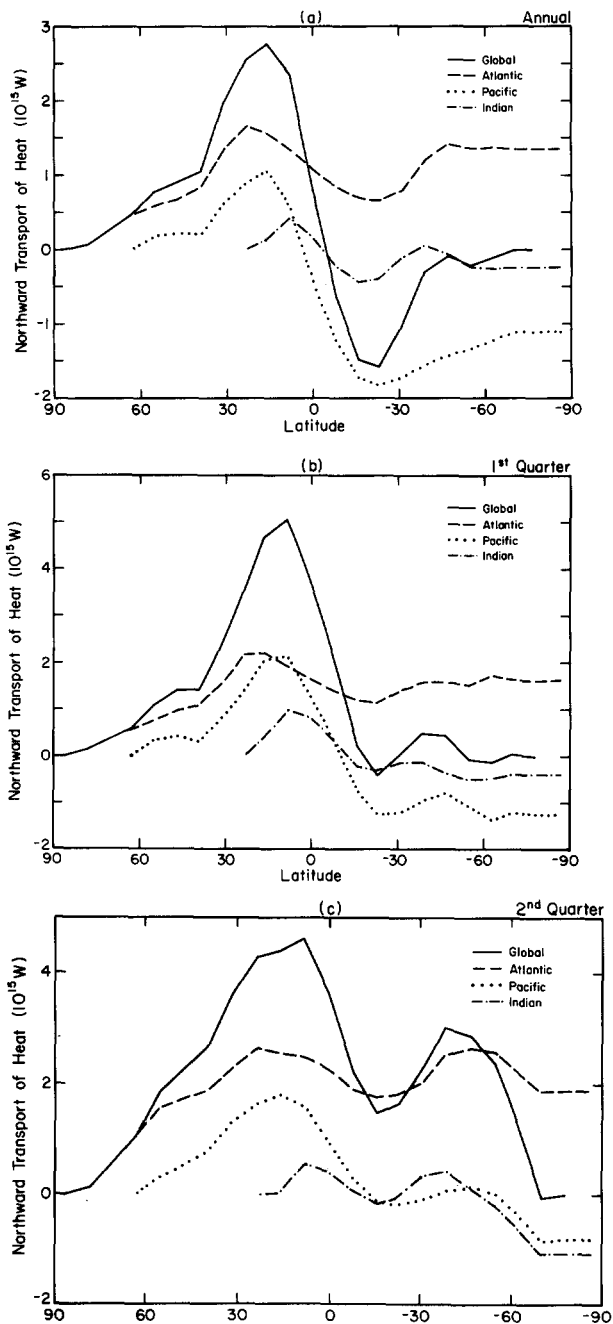


Fig. 11. Northward oceanic heat transports for the ocean basins and the global ocean as generated by the climate model for (a) the annual average and (b)–(e) for the quarters of the year.

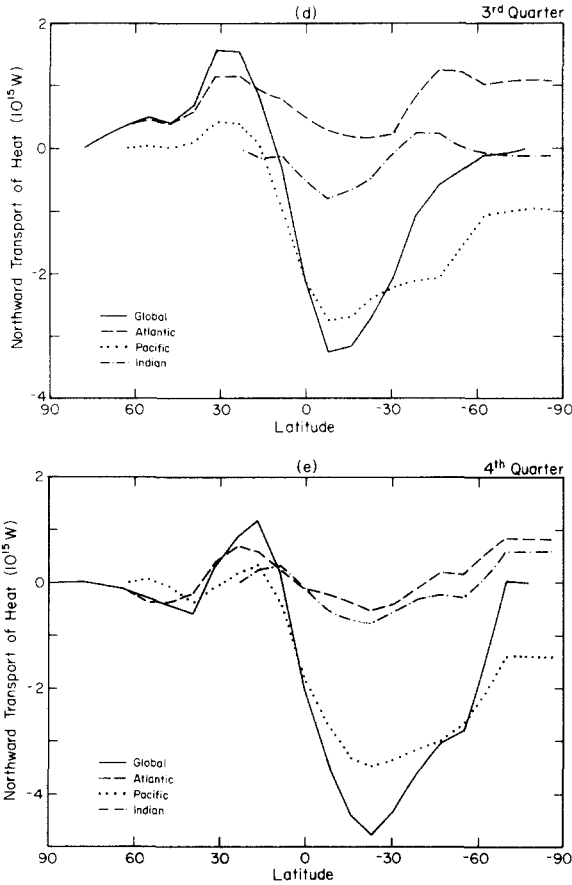


Fig. 11 (continued).

11a. For the global ocean the maximum poleward transports are approximately twice the annual average and occur during the winter seasons in both the Northern and Southern Hemispheres. The maximum transport attained is 5.0 PW at 10–15°N during the Northern Hemisphere winter. The cross-equatorial global transport is southward during the third and fourth quarters and northward during the first and second quarters. The net annual transport across the equator is northward. The maximum southward transport is 4.8 PW at 20–25°S during the fourth quarter.

It is useful to compare these seasonal global transports with other studies. Oort and Vonder Haar (1976) used the residual method to calculate seasonal heat transports for the Northern Hemisphere and Meehl et al. (1982) used a global ocean model to obtain transports for both hemispheres. Figure 12

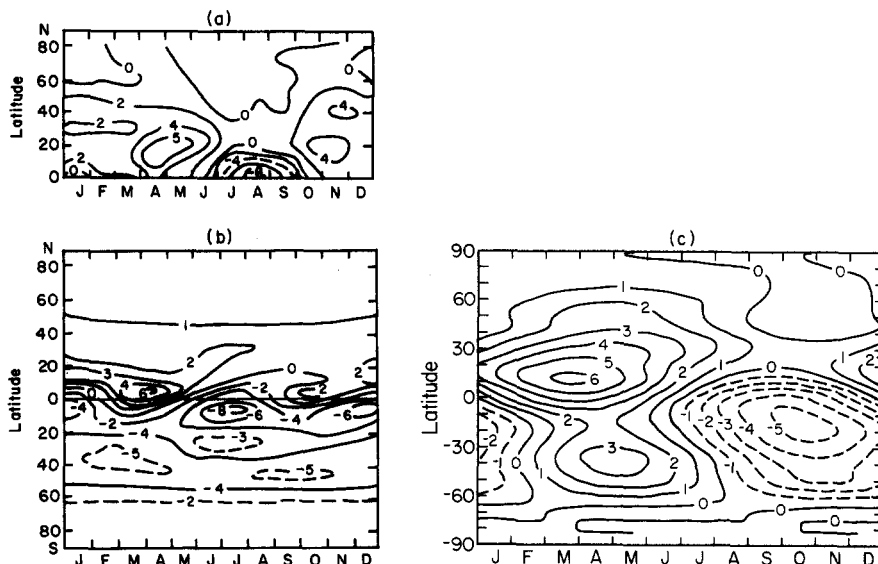


Fig. 12. Annual cycle of oceanic northward heat transports (PW) for (a) Oort and Vonder Haar, 1976 (b) Meehl et al., 1982 and (c) the climate model.

shows the comparison of the climate model results with these two studies. All three show a maximum northward transport of 5–6 PW in the second quarter with the climate model attaining a maximum in March and the Oort and Vonder Haar transports in April. The latitude at which this maximum occurs varies between 5 and 20°N for the three different studies. The maximum southward transport occurs about 2 months later for the climate model than for the other two and it is about 10° farther south for the climate model.

One of the principal concerns with the climate model results is the large northward transport between 30 and 50° in the Southern Hemisphere centered on the second quarter of the year. This could be anticipated from Fig. 11a in which the net global transport is near zero south of 40°S. Hence the negative transports south of 40°S in the last two quarters would have to be balanced by northward transport during the rest of the year. One reason for this result may be the net annual positive flux of heat into the ocean in most areas south of 40°S (see Fig. 5a). This excess heat must be transported northward out of the region.

The climate model and Oort and Vonder Haar transports do not show the semiannual component in the tropics as obtained by Meehl et al. (1982). When Meehl et al. ran their model using only the first harmonic of the wind

stress forcing, their equatorial transports corresponded with the transports of the climate model and Oort and Vonder Haar—southward during the Northern Hemisphere summer and fall, and northward during the winter and spring. They concluded that the semiannual features of tropical heat transport resulted from using 12 monthly values of the observed wind stress forcing rather than just the first harmonic. They also concluded that the heat transports from the ocean model of Bryan and Lewis (1979) did not show the semiannual tropical heat transport because it did not include the semiannual harmonic of wind stress forcing.

Each ocean basin has its own distinct transport characteristics. The Pacific is similar to the global pattern in that the latitude of maximum northward and southward transports coincide and have the same direction for each season. There is a net northward cross-equatorial transport in the last two quarters. The maximum northward Pacific transport during the first quarter is 2.1 PW, about twice the annual average. The maximum southward transport in the third quarter is 2.8 PW, which is about 50% greater than the annual average.

The transports in the Atlantic differ from the global pattern since the annual mean transport is northward at all latitudes in the Atlantic. Only during the fourth quarter of the year does the Atlantic transport become southward. The Indian Ocean transport roughly approximates the Pacific transport but has a much smaller amplitude.

The differences between the January and July transports for the Atlantic and Pacific Oceans are consistent with the results of Bryan (1982b) as obtained from the numerical ocean model of Bryan and Lewis (1979). Figure 13 shows the comparison of the climate model's heat transport for January and July in the Atlantic and Pacific with those from the Bryan and Lewis ocean model. In both the Atlantic and Pacific Oceans, the latitude of maximum northward transport shifts northward from January to July. In July, both models show a maximum at about 30°N for both ocean basins. The Northern Hemisphere maxima for the ocean model in January are about 5–10° south of those of the climate model.

Both the ocean and the climate model indicate that there is almost no change in the magnitude of the maximum northward transport between July and January in the Atlantic. For the climate model the maximum northward transport is 1.7 PW in both months while the ocean model shows a decrease from 0.7 PW to 0.6 PW between January and July. The behavior in the Pacific is quite different. Both models show a decrease in the maximum northward transport of about 50% between January and July from 1.7 to 0.8 PW for the climate model and from 1.2 to 0.6 PW for the ocean model. These results indicate that there is greater annual variation in the transports in the Pacific than in the Atlantic.

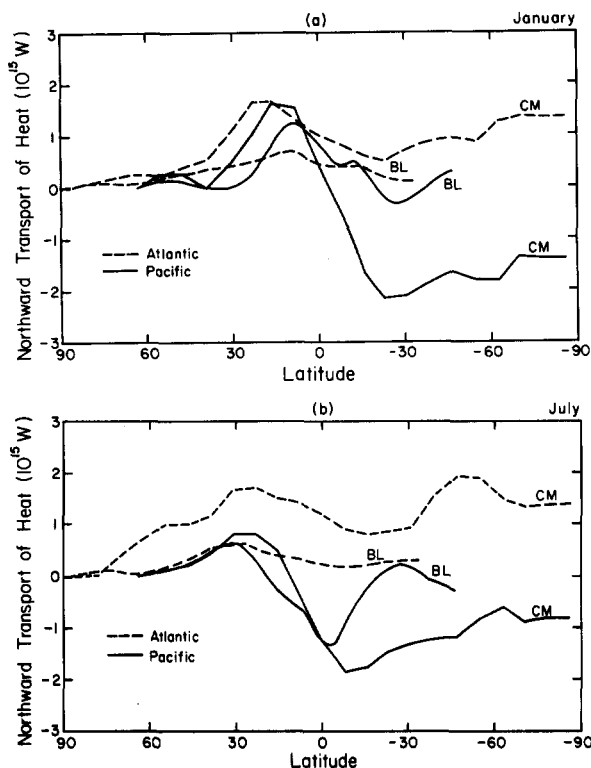


Fig. 13. Comparison of heat transports from the Bryan and Lewis model and the climate model for the Pacific and the Atlantic: (a) January and (b) July.

The annual variation of the climate model transports can also be seen in Fig. 11. The maximum annual northward transport (Fig. 11a) is 1.1 and 1.7 PW for the Pacific and Atlantic, respectively. For the Atlantic, the maximum northward transport in the second quarter is about 1 PW greater than the annual mean, and in the fourth quarter about 1 PW less than the annual mean. Hence the amplitude of the seasonal variations is about 50–60% of the annual mean. The amplitude of the seasonal variations for the Pacific is about 85% of the annual mean.

The seasonal variations calculated from the climate model are similar to those of Bryan (1982b) calculated from the ocean model. He found that the seasonal variations in heat transport were due primarily to seasonal wind variations. These variations were much more pronounced in the Pacific than in the Atlantic. The transports in the Atlantic are dominated by the thermohaline circulation and not significantly affected by wind variations. In the Pacific, however, the Northern Hemisphere trades strengthen from December to February and the heat transport reverses over a large area.

6. SUMMARY

The seasonal oceanic heat transports for each of the three ocean basins and the global ocean have been calculated using radiation and heat flux data at the air-sea interface. This is an extension of the annual heat transport calculations of MRT which used the same atmospheric general circulation model on an $8^\circ \times 10^\circ$ grid. The diagnostics are from a 1-y simulation using this model. Since the heat storage in the deep ocean in eq. 6 is not known and since our calculation of the ocean transports requires this component, the rate of change of deep ocean storage was assumed to be spatially uniform.

The results show northward transport of heat in January and July in the Atlantic Ocean, a result which is consistent with that of Bryan and Lewis (1979). The results also agree with those of Bryan and Lewis (1979) for the Pacific Ocean in which they show northward equatorial transport in January and southward in July. The maximum global northward transport which occurs in the first quarter is approximately twice that of the annual mean transport, a result which is consistent with that of Oort and Vonder Haar (1976). The amplitude of the seasonal variations of the maximum northward transport in the Pacific is approximately equal to 80–90% of the annual mean transport, but the amplitude of the seasonal variations in the Atlantic is only about 50–60% of the annual mean. These results agree with those of Bryan (1982b). The semiannual pattern of equatorial transport from the ocean model of Meehl et al. (1982) was not apparent in the present study.

The seasonal heat transports calculated from the diagnostics of the climate model are in good agreement with some of the limited set of calculations using other methods. The maximum values, however, appear to be larger than those calculated using direct methods.

As suggested in MRT, further improvements in the climate model are likely to improve the accuracy of both the seasonal and annual oceanic heat transports. In addition, replacing our assumption about the deep ocean storage with actual climatological data will improve the accuracy of the seasonal oceanic heat transports.

REFERENCES

- Ballis, D.J., 1973. Monthly mean bathythermograph data from Ocean Weather Station "Papa". Scripps Inst. Oceanogr. Ref. Series 73-5, 101 pp.
- Bryan, K., 1982a. Poleward heat transport by the ocean: observations and models. *Annu. Rev. Earth Planet Sci.*, 10: 15–38.
- Bryan, K., 1982b. Seasonal variation in meridional overturning and poleward heat transport in the Atlantic and Pacific Oceans: a model study. *J. Mar. Res.*, 40: 39–53.
- Bryan, K. and Lewis, L.J., 1979. A water mass model of the world ocean. *J. Geophys. Res.*, 84: 2503–2517.

- Gordon, A.L., 1982. Southern Ocean Atlas. Columbia Univ. Press, New York, 248 plates, 34 pp.
- Hansen, J., Russell, G., Rind, D., Stone, P., Lacis, A., Lebedeff, S., Ruedy, R. and Travis, L., 1983. Efficient three dimensional global model for climate studies: Models I and II. *Mon. Weather Rev.*, 111: 609–662.
- Meehl, G.A., Washington, W.M. and Semtner, A.J., 1982. Experiments with a Global Ocean Model Driven by Observed Atmospheric Forcing. *J. Phys. Oceanogr.*, 12: 301–312.
- Miller, J.R., Russell, G.L. and Tsang, L-C., 1983. Annual oceanic heat transports computed from an atmospheric model. *Dyn. Atmos. Oceans*, 7: 95–109.
- Oort, A.H. and Vonder Haar, T.H., 1976. On the observed annual cycle in the ocean–atmosphere heat balance over the Northern Hemisphere. *J. Phys. Oceanogr.*, 6: 781–800.
- Slingo, J.M., 1982. Study of the Earth’s radiation budget using a General Circulation Model. *Q. J. R. Meteorol. Soc.*, 108: 379–405.
- Weare, B.C., 1983. Interannual variation in net heating at the surface of the tropical Pacific Ocean. *J. Phys. Oceanogr.*, 13: 873–885.